

# Phosphatidylinositol 3-kinase Inhibitor (PIK75) Containing Surface Functionalized Nanoemulsion for Enhanced Drug Delivery, Cytotoxicity and Pro-apoptotic Activity in Ovarian Cancer Cells

Meghna Talekar · Srinivas Ganta · Amit Singh · Mansoor Amiji · Jackie Kendall · William A. Denny · Sanjay Garg

Received: 15 March 2012 / Accepted: 21 May 2012 / Published online: 1 June 2012  
© Springer Science+Business Media, LLC 2012

## ABSTRACT

**Purpose** Ovarian cancer is a debilitating disease, which needs multi-pronged approach of targeted drug delivery and enhanced efficacy with the use of combination therapeutics. In this study, we have examined the anticancer activity of PIK75 incorporated in surface functionalized nanoemulsions for targeted delivery to SKOV-3 cells. A pro-apoptotic molecule C<sub>6</sub>-ceramide was also co-delivered to augment therapeutic efficacy.

**Methods** EGFR and FR functionalized nanoemulsions incorporating PIK75 and C<sub>6</sub>-ceramide were characterized for particle size, surface charge, entrapment efficiency and morphology. Fluorescence and quantitative uptake studies were conducted in SKOV-3 cells to determine intracellular distribution. Cell viability was assessed using MTT assay while mechanism of cytotoxicity was evaluated using caspase-3/7, TUNEL and hROS assay.

**Results** Cytotoxicity assay showed 57% decrease in IC<sub>50</sub> value of PIK75 following treatment with EGFR targeted nanoemulsion and 40% decrease following treatment with FR targeted nanoemulsion. Combination therapy with PIK75 and ceramide enhanced the cytotoxicity of PIK75 compared to therapy with individual formulations. The increase in cytotoxicity was attributed to increase in cellular apoptosis and hROS activity.

**Conclusion** The results of this study showed that the targeted system improved cytotoxicity of PIK75 compared to the non-targeted system. Combination therapy with ceramide augmented PIK75's therapeutic activity.

**KEY WORDS** C<sub>6</sub>-ceramide · EGFR · folate · nanoemulsion · ovarian cancer · phosphatidylinositol 3-kinase inhibitor

## ABBREVIATIONS

CER	ceramide
EGFR	epidermal growth factor receptor
FR	folate receptor
NE	nanoemulsions
PI3K	Phosphatidylinositol 3-kinase
PIP <sub>2</sub>	Phosphatidylinositol 4, 5-diphosphate
PIP <sub>3</sub>	Phosphatidylinositol 3, 4, 5-triphosphate

## INTRODUCTION

Ovarian cancer is the fifth leading cause of cancer related death in women and is one of the most deadly forms of gynecological cancer (1). It is often treated by chemotherapy, combined with surgery or radiotherapy. First line chemotherapeutic agents fail to provide remission in approximately 70% of patients and about 40–50% of women who experience remission are likely to relapse within 3 years of treatment demonstrating a need to develop newer cytotoxic agents in order to provide patients with a greater range of treatment options.

M. Talekar · S. Garg  
School of Pharmacy, Faculty of Medical & Health Sciences  
The University of Auckland, Private Bag 92019  
Auckland, New Zealand

S. Ganta  
Nemucore Medical Innovations, Inc.  
Worcester, Massachusetts 01608, USA

A. Singh · M. Amiji  
Department of Pharmaceutical Sciences, School of Pharmacy  
Northeastern University, 140 The Fenway Building  
360 Huntington Ave., Boston, Massachusetts 02115, USA

J. Kendall · W. A. Denny  
Auckland Cancer Society Research Centre  
Faculty of Medical & Health Sciences, The University of Auckland  
Private Bag 92019  
Auckland, New Zealand

S. Garg (✉)  
School of Pharmacy & Medical Sciences  
University of South Australia (UniSa), GPO Box 2471  
Adelaide, South Australia 5001, Australia  
e-mail: Sanjay.Garg@unisa.edu.au

A major target in ovarian cancer is the phosphatidylinositol 3-kinase (PI3K) enzyme p110  $\alpha$ , an isoform which is frequently activated in human colorectal, ovarian, breast and liver cancers and is a major target for small-molecule inhibitors (2–5). PI3Ks are a family of lipid kinases which catalyze the phosphorylation of the 3-hydroxyl position of the inositol ring of phosphatidylinositol 4, 5-diphosphate (PIP<sub>2</sub>) to give the second messenger molecule phosphatidylinositol 3, 4, 5-triphosphate (PIP<sub>3</sub>) which allows PI3K to couple with downstream effectors such as Akt which leads to inhibition of caspase activity preventing apoptosis. Since other isoforms of PI3K also have critical cellular functions, compounds that specifically inhibit p110  $\alpha$  have been a major goal as potential anticancer agents (6–9).

PIK75 (Fig. 1) is a preferential PI3K p110  $\alpha$  inhibitor (enzyme IC<sub>50</sub> p110  $\alpha$  - 7.8  $\pm$  1.7 nM; p110  $\beta$  - 343  $\pm$  23 nM; p110  $\delta$  - 907  $\pm$  32 nM) (10,11) which shows potent inhibition of cellular proliferation (IC<sub>50</sub>s of 69 nM in NZB5 medulloblastoma cells and 66 nM in NZOV9 ovarian tumor cells) (12) and has demonstrated activity in a HeLa human cervical cancer xenograft model (13). PIK75 also inhibits PI3K activation in ovarian cancer cells (14). However the development of PIK75 as a drug has been limited by its poor aqueous solubility likely due to its high melting point (216°C) and high log *P*<sub>octanol/water</sub> (3.84). It is soluble in a range of organic solvents but not at concentrations well tolerated in animals and thus has only been dosed as a suspension formulation (12).

PIK75 is a good candidate for incorporation into nano-size systems for enhanced delivery and in this paper we discuss the development of nanoemulsion preparations of this drug. Nanoemulsions are nanoscale droplets (size range of 20–200 nm) of one immiscible liquid phase dispersed within another and stabilised using an appropriate emulsifier. They are often formulated as oil-in-water emulsions where the lipophilic compound is

solubilized in the lipid core. This system offers several advantages over other delivery systems including enhanced solubility of poorly water soluble drugs, avoiding pain associated with the intravenous administration of anticancer agents and feasibility of being scaled up. Nanoemulsions have been used for the delivery of several poorly water-soluble anticancer agents some of which have been functionalized to enhance circulation time or improve tumor uptake (15–19). Only a few studies, however, have reported targeted drug delivery using nanoemulsions (20). Hence, we investigated the effect of using epidermal growth factor receptor (EGFR) and folate receptor (FR) targeted nanoemulsions on the cytotoxicity of PIK75 in this study.

The first approach uses a peptide that binds specifically to the epidermal growth factor receptor (EGFR), a member of the ErbB family of tyrosine kinase receptors which are over-expressed in many solid tumors. Many papers have reported the development of EGFR targeted nanoparticles for site-specific delivery of anticancer agents (21,22). Likewise folic acid has often been incorporated in nanoparticulate systems for the targeted delivery of anticancer agents (23), antisense oligonucleotides (24), folate conjugated protein toxins (25) and folic acid derivatized diagnostic agents (26). Folate receptors (FRs) are also overexpressed in several human cancers including ovarian, endometrial, colorectal, breast, lung and renal carcinoma. Furthermore, as a tumor progresses, the density of FR on cell surface is also known to increase. However, often effective cytotoxicity cannot be attained by targeted delivery of anticancer agents to tumor tissues. In this situation targeting tumor cells with a combination of cytotoxic agents would be an effective strategy. One such strategy is the co-administration of cytotoxic agents with ceramide.

Ceramides are short chain sphingolipids which inhibit pro-survival pathways, induce mitochondrial dysfunction and stimulate caspase activity resulting in DNA fragmentation and cell death (27). Previous work has shown that exogenous administration of ceramide reinstates the apoptotic signal and resensitizes cancer cells to anticancer therapy (28). Combination therapy of paclitaxel and ceramide in SKOV-3-cells and tumor models has shown improved therapeutic efficacy, including overcoming higher apoptotic threshold in resistant phenotype (28,29). Hence, we have also investigated the effect on PIK75's cytotoxicity by co-administering ceramide and PIK75.

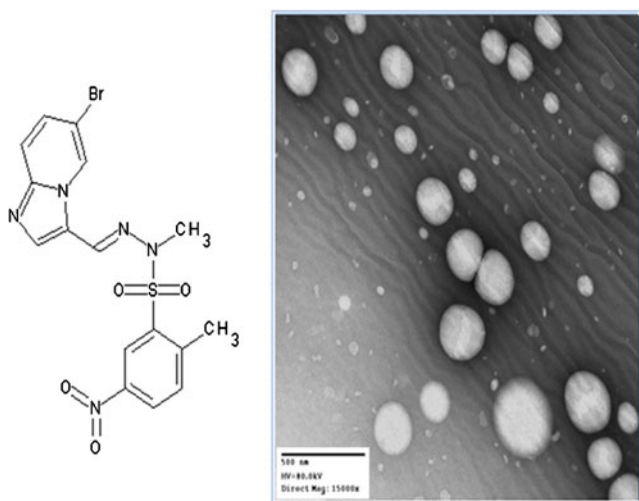


**Fig. 1** Chemical structure of phosphatidylinositol 3-kinase Inhibitor (PIK75) and transmission electron micrograph of PIK75 containing nanoemulsion.

## MATERIALS AND METHODS

### Materials

Phosphatidylinositol 3-kinase inhibitor (PIK75) was synthesized at the Auckland Cancer Society Research Centre

using published routes (12,13). C<sub>6</sub>-Ceramide (N-hexanoyl-D-erythro-sphingosine) was purchased from Avanti Polar Lipids (Alabaster, AL) and EGFR binding peptide YHWY-GYTPQNVI with a linker sequence GGGGC was obtained from Tufts University, Boston, MA. 1,2-distearoyl-*sn*-glycero-3-phosphoethanolamine-N-[maleimide(polyethylene glycol)-2000] (ammonium salt) (DSPE-PEG<sub>2000</sub> maleimide) was purchased from Laysan Bio Inc., (Arab, AL) and 1,2-distearoyl-*sn*-glycero-3-phosphoethanolamine-N-[methoxy-(polyethyleneglycol)-2000] (DSPE-PEG<sub>2000</sub>) was provided by Genzyme Corporation (Cambridge, MA). Flax seed oil was provided by Jedwards International (Quincy, MA). Egg phosphatidylcholine (Lipoid® E-80) was acquired from Lipoid GMBH (Ludwigshafen, Germany) and fluorescent probe, 6-((N-(7-nitrobenz-2-oxa-1,3-diazol-4-yl)amino)hexanoyl)Sphingosine (NBD C<sub>6</sub>-Ceramide) was obtained from Invitrogen (Eugene, Oregon). Cysteine, N, N'-dicyclohexylcarbodiimide and 3-[4, 5-dimethylthiazolyl]-2, 5-diphenyltetrazolium bromide (MTT reagent) were procured from Sigma Chemicals (St. Louis, MO). SKOV-3 human ovarian adenocarcinoma cells were obtained from American Type Culture Collections (Manassas, VA). BCA protein assay kit and chemiluminescence substrate were obtained from Thermo Scientific (Rockford, IL). ApoONE Homogenous Caspase-3/7 assay kit and the DeadEnd Colorimetric apoptosis detection system (TUNEL assay) were purchased from Promega (Madison, WI). hROS detection kit was acquired from Cell Technology (CA, USA).

All other chemicals and solvents were of analytical reagent grade and were used without further purification.

### Synthesis of EGFR-PEG<sub>(2000)</sub>-DSPE Conjugate

EGFR specific peptide, YHWYGYTPQNVI designated as GE11 was used to prepare EGFR functionalized nanoemulsions to target SKOV-3 ovarian tumor cells over expressing EGFR. The GE11 peptide was originally synthesized and screened as an EGFR specific peptide by Zonghai Li and colleagues (30,31). For this study the GE11 peptide with a spacer sequence of GGGGC was synthesized at Tufts University Core Facility, Boston, MA. The carboxyl group of terminal cysteine of the peptide was reacted with the maleimide of PEG<sub>2000</sub>-DSPE to form the construct by adding EGFR peptide to DSPE-PEG<sub>(2000)</sub>-maleimide (MW - 2942) dissolved in HEPES buffer (pH 7.4) at 1:1 molar ratio while mixing under N<sub>2</sub> at 4°C for 24 h. The peptide conjugate was then purified by dialysis (3.5 kDa), lyophilized and characterized by NMR spectroscopy.

### Synthesis of FA-cys-PEG<sub>(2000)</sub>-DSPE Conjugate

Folic acid (FA) was used in the preparation of folate-functionalized nanoemulsions to target SKOV-3 tumor cells

over expressing folate alpha receptors. FA-cys-PEG<sub>(2000)</sub>-DSPE conjugate was prepared by adding 8.24 mg of cysteine to 100 mg DSPE-PEG<sub>(2000)</sub>-maleimide dissolved in 25 ml of HEPES buffer. The sample was then incubated overnight at 4°C under N<sub>2</sub> then dialyzed (3.5 kDa cut-off) to remove excess cysteine and lyophilized. 51 mg of this lyophilized complex was added to FA (13 mg) dissolved in 6 ml of anhydrous dimethyl sulfoxide (DMSO). Pyridine (3 ml) was then added followed by 16 mg of N, N'-dicyclohexylcarbodiimide and the reaction was stirred at room temperature for 4 h. The samples were evaporated to dryness under vacuum to remove the pyridine and DMSO and resuspended in 50 mL water, dialyzed, freeze dried and characterized by NMR spectroscopy.

### Preparation of PIK75-nanoemulsion Formulations

PIK75 (7 mg) in chloroform was added to flax seed oil (1.0 g) following which N<sub>2</sub> was blown in the sample to evaporate the solvent and obtain the drug in lipid phase. The aqueous phase was prepared by dissolving DSPE-PEG<sub>2000</sub> (15 mg) and egg lecithin (120 mg) in deionized water (4 ml) by stirring for 30 min. The lipid and aqueous phases were heated separately to 70°C for 5 min and then the aqueous phase was mixed to the lipid phase to prepare a coarse emulsion. This was ultrasonicated at 30% amplitude and 50% duty cycle for 5 min using Vibra-Cell VC 505 ultrasound instrument (Sonics and Materials, Inc., Newton) to obtain the PIK75 nanoemulsion (PIK75 NE).

PIK75 formulations containing targeted nanoemulsions were prepared similarly, except that EGFR-PEG<sub>2000</sub>-DSPE (2.5 mg) or FA-cys-PEG<sub>2000</sub>-DSPE (7.94 mg) conjugate was added to the aqueous phase of formulation to form the EGFR targeted nanoemulsion (PIK75 NE-EGFR) or the FA targeted PIK75 nanoemulsion (PIK75 NE-FA), respectively.

The C<sub>6</sub>-ceramide containing nanoemulsion (CER NE) and targeted nanoemulsions (CER NE-EGFR and CER NE-FA) were also prepared using a similar procedure but ceramide (40 mg) was added to the organic phase instead of PIK75. For control experiments, blank nanoemulsions without the drugs were prepared in a similar manner.

### Characterization of Nanoemulsions

#### Particle Size and Zeta Potential

The particle size, polydispersity index (PDI) and zeta potential of the nanoemulsions were determined by photon correlation spectroscopy using Zetasizer Nano ZS (Malvern, UK) at a 90° fixed angle and at 25°C. The samples were diluted with milli-Q water to a suitable scattering intensity prior to the measurement and 1 ml aliquot was used to measure the particle size

and PDI. Refractive index value of 1.45 was used for these measurements.

Average surface charge of nanoemulsion oil droplets was determined by taking 1 ml diluted nanoemulsions in electrophoretic cell and the measurements were done at 25°C under electric field strength of 23.2 V/cm.

### Transmission Electron Microscopy

Transmission electron microscopy (TEM) images were obtained to assess the size and morphology of the formulations. For this, 10 µL of the diluted nanoemulsion was placed on the Formvar-coated copper grids (Electron Microscopy Science, Hatfield, PA) and negatively stained with 50 µL of 1% (w/v) uranyl acetate for 10 min. A Whatman filter paper was used to drain excess liquid, the grids were allowed to air-dry and were observed with a JEOL 100X transmission electron microscope (Peabody, MA).

### PIK75 HPLC Analysis

A HPLC analysis was used to determine PIK75 entrapment efficiency in the non-targeted and targeted nanoemulsions. A Waters LC system (model 2487, Waters Corporation, Milford) comprising of a quaternary pump, an autosampler, and UV-detector was used for PIK75 analysis. The LC system was interfaced with Empower software for instrument control, data acquisition and processing. Separation was performed on a reverse phase C18 column (4.6 mm × 150 mm, 5 µm, Agilent Zorbax column, USA) using a guard C18 pre-column with security guard cartridges (20 mm × 4 mm, 5 µm, Phenomenex, USA). The mobile phase consisted of solvent A (80% acetonitrile in Milli-Q water) and solvent B (45 mM ammonium formate, pH 3.5), which was circulated at a flow rate of 1 ml/min with a gradient method. The gradient used was: 0-15 min 25% of solvent A; 15-17 min 95% solvent A; 17-20 min 25% of solvent A. Samples were injected at 30 µl of injection volume and analyzed at 270 nm.

### Drug Assay and Entrapment Efficiency

PIK75 concentration in the formulations was determined by extracting PIK75 from nanoemulsions using acetonitrile followed by HPLC analysis. 5 ml of acetonitrile was added to the nanoemulsion (0.15 ml), samples were vortexed, sonicated and centrifuged (1,000 rpm, 10 min). The supernatant was collected, diluted with the mobile phase and injected on HPLC for PIK75 assay.

PIK75 encapsulation efficiency was determined by an ultrafiltration method using centrifugal filter devices (molecular weight, cut-off 3,000 Daltons) (Centricorn, Millipore, Bedford, MA). In this method, the hydrostatic pressure

against the membrane allowed the aqueous phase to separate from the lipid phase. Nanoemulsion sample (1 ml) was placed in the upper donor chamber and the unit was centrifuged at 3,500 rpm for 15 min. Drug incorporated in the lipid phase remained in the donor chamber and the aqueous phase moved into the recovery chamber. The PIK75 in the aqueous phase was estimated using HPLC. PIK75 entrapment efficiency was determined by subtracting the encapsulation efficiency value from the PIK75 assay value.

### Cellular Uptake of Fluorescently Labeled Nanoemulsions

Fluorescently labeled nanoemulsions were prepared by incorporating NBD-C<sub>6</sub>-ceramide (0.05%w/v) in the lipid phase and preparing the nanoemulsion as described previously. SKOV-3 cells were plated on glass coverslips in six-well microplates and incubated with 50 µl of NBD-C<sub>6</sub>-ceramide nanoemulsions diluted with 2 ml of RPMI media per well. At pre-determined time intervals (15, 30 and 60 min), the cells were washed with RPMI and the coverslips were placed on glass slides prior to imaging. Brightfield and fluorescence images were obtained at 20x magnification on an Olympus fluorescence microscope.

### Quantitative Cellular Uptake of PIK75 from Nanoemulsions

Approximately  $4 \times 10^6$  SKOV-3 cells were cultured in T-150 flasks and the cells were allowed to adhere by incubating them overnight. An equivalent of 10 µM of PIK75 in formulations (solution, non-targeted, EGFR and FR targeted nanoemulsions) were diluted with RPMI and added to each of the flasks. After 6 h of incubation, the flasks were washed twice with 1% PBS solution to ensure that excess non-internalized formulation was removed. Cell lyses buffer was added to lyse the cells; the lysate was collected, and centrifuged at 13,000 rpm for 15 min at 4°C. The supernatant was collected and the protein concentration was determined using bicinchonic acid (BCA) protein assay kit. Intracellular PIK75 uptake was estimated using above described HPLC analysis and PIK75 concentration was determined relative to the total amount of protein in the cell.

To prepare the sample for measurement, 300 µL of ice-cold acetonitrile was added to the cell lysate in order to precipitate the protein and incubated at -20°C for 30 min. The samples were then centrifuged for 15 min at 13,000 rpm and 4°C. The supernatant was extracted, diluted with the mobile phase and the concentration of PIK75 was determined using HPLC. The PIK75 concentration in PIK75 solution, PIK75 nanoemulsion and targeted nanoemulsions was determined by extrapolating the readings obtained from the standard curve. The final

PIK75 concentration was reported as  $\mu\text{g}$  of the drug per  $\text{mg}$  of total cellular protein.

### Cytotoxicity with Single and Combination Therapy

The cytotoxicity studies were carried out by using graded concentrations of PIK75 as single and as combination therapy with ceramide. PIK75 stock concentrations (10, 50, 500  $\mu\text{M}$ ) were prepared by diluting the PIK75 solution (PIK75 in DMSO), PIK75 NE, PIK75 NE-EGFR and PIK75 NE-FA in RPMI. These stock solutions were further diluted with RPMI to obtain graded concentrations (10, 100, 1000, 10,000, 100,000  $\text{nM}$ ) of PIK75. Likewise ceramide stock concentration (250, 1000  $\mu\text{M}$ ) were prepared and further diluted with RPMI to obtain graded concentrations (1, 5, 10, 20, 40, 60, 80, 100  $\mu\text{M}$ ) of ceramide.

For cytotoxicity testing, 3,000 cells per well were cultured in 96 well plates and allowed to adhere overnight. RPMI growth media was used as a negative control (0% cell death) and poly(ethyleneimine), a cationic cytotoxic polymer at a concentration of 0.25  $\text{mg}/\text{ml}$  (molecular weight 10  $\text{kDa}$ ) was used as a positive control (100% cell death). Each of the graded concentration of PIK75 was tested with eight replicates and the plates were incubated for 72 h. The media was then replaced with 50  $\mu\text{L}$  of MTT (2.0  $\text{mg}/\text{ml}$  in RPMI) and the plates were incubated for 3 h to enable viable cells to reduce the tetrazolium compound into formazan dye. The formazan crystals were then dissolved in 200  $\mu\text{L}$  of DMSO and the plates were rocked gently for 5–10 min to ensure that all the crystals were dissolved. Plates were read at 570  $\text{nm}$  using a Bio-Tek Synergy HT plate reader (Winooski, VT) and the percentage cell viability was measured relative to the negative control. The  $\text{IC}_{50}$  value for PIK75 and ceramide as single agents and in combination was determined using GraphPad Prism 5 software by sigmoidal curve fitting method.

### Quantitative and Qualitative Apoptotic Analysis

#### TUNEL Assay

Qualitative analysis of apoptotic activity following treatment with PIK75 and ceramide formulations was determined by terminal transferase dUTP nick end labeling (TUNEL) assay. Cells were grown on glass coverslips in 6-well microplates (20,000 cells per well) and they were treated with PIK75 (100  $\text{nM}$ ) and ceramide (10  $\mu\text{M}$ ) as single agents and in combination; in solution as well as in formulations. After 48 h of treatment the cells were fixed with 10% formalin in PBS for 25 min and permeabilized with 0.2% Triton X-100 in PBS for 5 min at room temperature. After washing with PBS, the coverslips were incubated with 100  $\mu\text{L}$  rTdT reaction mixture and kept at 37°C, 5%

$\text{CO}_2$  for 60 min. Cover slips were incubated with sodium citrate buffer for 15 min at room temperature and washed with PBS to remove the unincorporated biotinylated nucleotides. The coverslips were then immersed in 0.3% hydrogen peroxide solution in PBS for 3–5 min to block endogenous peroxidase. After the washing, coverslips were incubated with 100  $\mu\text{L}$  of diluted streptavidin-HRP (1:500 in PBS) for 30 min. The cells were washed in PBS followed by incubation with 100  $\mu\text{L}$  of freshly prepared DAB solution. The coverslips were then washed several times in deionized water, mounted on glass slides and observed under a light microscope.

#### Caspase-3/7 Activity Measurements

SKOV-3 cells were plated in 96 well microplates at a density of 20,000 cells per well. After overnight incubation the cells were treated with PIK75 (100  $\text{nM}$ ) and ceramide (10  $\mu\text{M}$ ) as single agents and in combination; in solution as well as in formulations. After 2 h the formulations were discarded and the cells were washed with RPMI and incubated with 100  $\mu\text{L}$  of media for 24 h. Apo-ONE Caspase 3/7 substrate (100  $\mu\text{l}$ ) solution with buffer was then added to each of the wells and the contents were mixed at 200–300 rpm for 2 h at room temperature. The fluorescence intensity was measured at an excitation wavelength of 490  $\text{nm}$  and an emission wavelength of 520  $\text{nm}$  using a Synergy HT microplate reader. Untreated cells were used as negative controls. For the determination of caspase activity blank formulation values were subtracted and fold increase in activity was calculated based on the activity measured from untreated cells.

#### Detection of Highly Reactive Oxygen Species Markers

For the detection of highly reactive oxygen species (hROS) markers 20,000 cells were seeded in 96 well plates and after overnight incubation the cells were treated with PIK75 (100  $\text{nM}$ ) as single agent and in combination with ceramide; in solution as well as nanoemulsion formulations. The cells were incubated with the PIK75 samples for 2 h and after 24 h the plates were washed with modified HBSS. APF dye (5  $\text{mM}$ ) was diluted with HBSS in a 1:10 ratio and 4  $\mu\text{L}$  of the diluted dye was added to 200  $\mu\text{L}$  of media for each well. The final concentration of the dye was adjusted to 10  $\mu\text{M}$ . The plates were then incubated at room temperature for 60 min. The fluorescence intensity was measured using Bio-Tek Instrument Synergy<sup>®</sup> HT microplate reader at an excitation/emission maxima of 490/515  $\text{nm}$ . Untreated cells and those treated with blank formulations were used as negative controls. For the determination of hROS activity blank values were subtracted and fold increase in activity

was calculated based on the activity measured from untreated cells.

## RESULTS

### Preparation of Nanoemulsion Formulations

Lipid-in-water nanoemulsions were prepared using flax seed oil as the lipid phase of the formulation in which PIK75 or ceramide was solubilized. Egg phosphatidylcholine was used in stabilizing the oil-droplets in aqueous phase by reducing the surface tension at the interfacial layer, whereas PEG<sub>(2000)</sub>DSPE provided steric stabilization. For surface functionalization EGFR- PEG<sub>(2000)</sub>DSPE and FA-PEG<sub>(2000)</sub>DSPE were synthesized based on maleimide chemistry. These conjugates were purified and characterized before being incorporated into the nanoemulsion formulation. They were added to the aqueous phase of the nanoemulsion, so that the DSPE phospholipid chain of the conjugate incorporated into the phospholipid monolayer on the oil droplet, while hydrophilic targeting moiety oriented into the aqueous phase of the formulation.

### Characterization of Nanoemulsion Formulations

Size distribution, surface charge and drug entrapment efficiency of all nanoemulsion formulations are shown in Table I. The blank NE showed an average particle size of  $164 \pm 22$  nm, the PIK75 NE showed an average particle size of  $197 \pm 2$  nm and both targeted NEs also showed similar particle sizes to the blank and PIK75 NE. CER NE's showed a particle size in the range of 147–183 nm. Polydispersity indices for all the nanoemulsions were between 0.1–0.3 indicating a narrow size distribution. Figure 1 depicts the TEM micrograph of nanoemulsion showing spherical morphology and uniform particle size. Zeta potential measurements indicated that all the nanoemulsion systems showed a surface charge in the range of (–) 50 to (–) 58 mV attributed to egg phosphatidylcholine incorporated

in the nanoemulsion. The zeta potential values for the PIK75 and ceramide formulations were similar to the Blank NE indicating that the drugs were confined to the lipid phase and did not adsorb to the interfacial layer to affect the surface charge.

Both non-targeted and targeted PIK75 nanoemulsions showed an entrapment efficiency of 79% (Table I) Although PIK75 has a  $\log P_{\text{octanol/water}}$  value of 3.84 and is soluble in a range of organic solvents; it has limited solubility in oils. Thus some of the PIK75 may have partitioned into the aqueous phase during the preparation of the nanoemulsions. In order to increase the percentage of entrapment, a higher quantity of PIK75 was incorporated in the organic phase but this led to drug precipitation. Hence the amount of PIK75 added to the nanoemulsions was limited to 7 mg, which provided an optimum entrapment of 79–82% in the lipid phase. C<sub>6</sub>-ceramide being a highly lipophilic molecule is freely soluble in many oils such as soybean oil, flax seed oil, pine nut oil and fish oil in the range of 80–100 mg/g oil. Based on our previous work on ceramide in our current study we observed 100% entrapment efficiency when 20 mg/ml ceramide nanoemulsions were prepared.

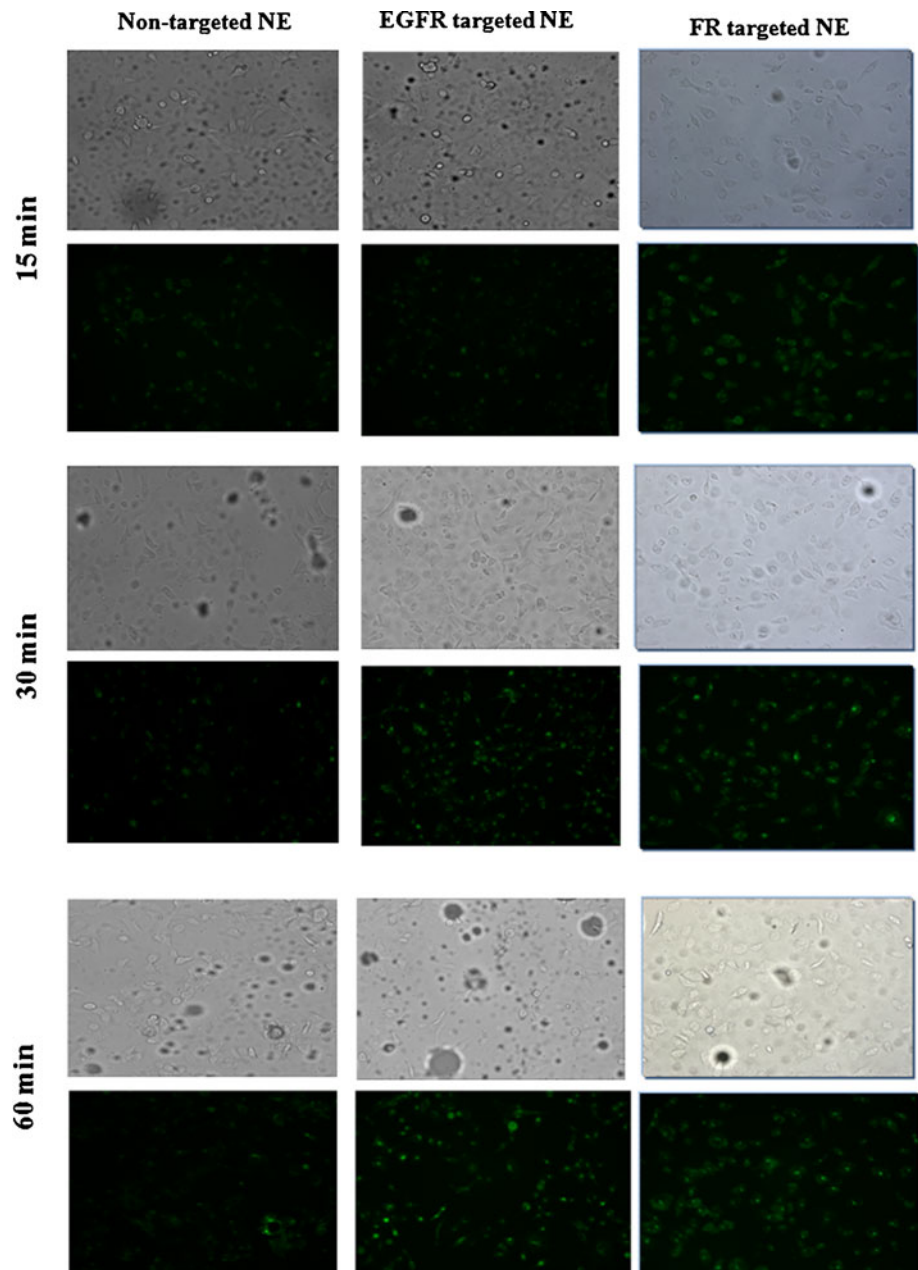
### Cellular Uptake of Fluorescently Labeled Nanoemulsion

Targeted and non-targeted NE formulations were prepared with NBD-C<sub>6</sub>-ceramide and their uptake in SKOV-3 tumor cells was monitored under fluorescence microscope (Fig. 2). Bright field images showed that morphology of the cells remained intact during the cell uptake study. All formulation systems showed intracellular uptake within 15 min of incubation. An increase in fluorescence intensity was observed with all the three systems as the period of incubation was increased. The targeted nanoemulsions showed greater fluorescence intensity at all time points compared to the non-targeted nanoemulsion. This difference may be due to receptor mediated endocytosis of the targeted nanoemulsions compared to non-specific endocytosis of non-targeted nanoemulsion. Furthermore, the hydrophilic PEG chains on

**Table I** Characterization of Nanoemulsion Formulations

Formulation	Average size (nm)	Polydispersity index	Zeta potential (mV)	Drug entrapment (%)
Blank NE	$164 \pm 22$	0.2	$-51.83 \pm 2.4$	–
PIK75 NE	$197 \pm 2$	0.2	$-54.93 \pm 0.8$	$79 \pm 4\%$
PIK75 NE-EGFR	$212 \pm 40$	0.1	$-57.23 \pm 2.8$	$79 \pm 4\%$
PIK75 NE-FR	$168 \pm 12$	0.2	$-55.50 \pm 1.5$	$79 \pm 4\%$
Ceramide NE	$147 \pm 18$	0.1	$-58.03 \pm 2.0$	100
Ceramide NE-EGFR	$205 \pm 18$	0.3	$-55.50 \pm 1.5$	100
Ceramide NE-FA	$183 \pm 61$	0.3	$-52.7 \pm 2.8$	100

**Fig. 2** Uptake of NBD  $C_6$ -ceramide incorporated non-targeted nanoemulsion (non-targeted NE), EGFR targeted nanoemulsion (EGFR targeted NE) and FR targeted nanoemulsion (FR targeted NE) in SKOV-3 cells after 15, 30 and 60 min of incubation. Brightfield and fluorescence images were acquired using a 20 $\times$  objective.



the surface of the non-targeted nanoemulsion may prevent interaction between the nanoemulsion and the SKOV-3 cells due to steric hindrance limiting uptake.

#### Quantitative Cellular Uptake of PIK75 from Nanoemulsion Formulations

The intracellular uptake of PIK75 in solution, targeted and non-targeted nanoemulsions was tested on SKOV-3 cells at an equivalent PIK75 dose of 10  $\mu$ M for 6 h. Figure 3 shows the concentration of PIK75 in  $\mu$ g relative to intracellular protein (mg). PIK75 NE and the targeted nanoemulsions showed a significantly greater uptake of PIK75 compared to

PIK75 solution ( $p < 0.05$ ). Likewise, both the targeted systems showed a significantly greater uptake of PIK75 compared to the non-targeted system. However a statistically significant difference was not observed between the two targeted systems.

#### Cytotoxicity with Single and Combination Therapy

The cytotoxicity of PIK75 and ceramide formulations in SKOV-3 cells was evaluated using the MTT assay. Figure 4 shows the percentage cell viability following treatment with PIK75 in solution, non-targeted NE and EGFR and FR targeted NE. The data was fitted using GraphPad Prism to

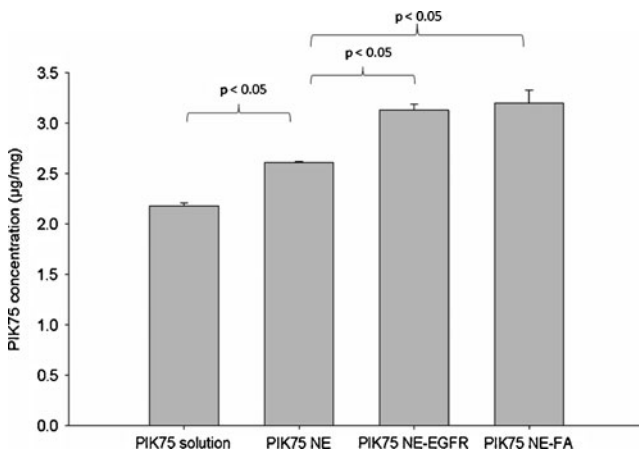


**Fig. 3** Quantitative intracellular uptake of PIK75 from PIK75 formulations after 6 h of incubation. Intracellular PIK75 concentration expressed as mg of protein from SKOV-3 cells. Each treatment represents  $n=3$ .

determine the  $IC_{50}$  values for each of the formulation systems. Table II shows the  $IC_{50}$  values of PIK75 and ceramide administered singly or in combination.

There was little difference in the  $IC_{50}$ s of PIK75 NE and PIK75 solution. This could be attributed to the presence of hydrophilic PEG chains on the surface of the nanoemulsion which may have posed a steric barrier affecting uptake of these nanoparticles. Treating the cells with PIK75 targeted systems was more effective showing 57% decrease with EGFR targeted nanoemulsion and 40% decrease with FR targeted nanoemulsion compared to PIK75 solution and PIK75 NE ( $p < 0.05$ ). In contrast to the PIK75 NE, the EGFR and FR targeted nanoemulsions would be taken up into the cells by receptor-mediated endocytosis leading to increased intracellular concentration and enhanced cytotoxicity. The FR targeted nanoemulsion showed 69% decrease in  $IC_{50}$  value of PIK75 compared to the EGFR targeted nanoemulsion ( $p < 0.05$ ).

**Fig. 4** Percentage cell viability of SKOV-3 cells as a function of (a) PIK75 concentrations when administered as a solution, PIK75 nanoemulsion (PIK75 NE), PIK75 EGFR targeted (PIK75 NE-EGFR) and folate targeted (PIK75 NE-FA) nanoemulsions, and (b) Percentage cell viability as a function of Ceramide concentrations when administered as a solution, Ceramide NE, Ceramide NE-EGFR and Ceramide NE-FA. The results represent mean  $\pm$  SD,  $n=8$ .

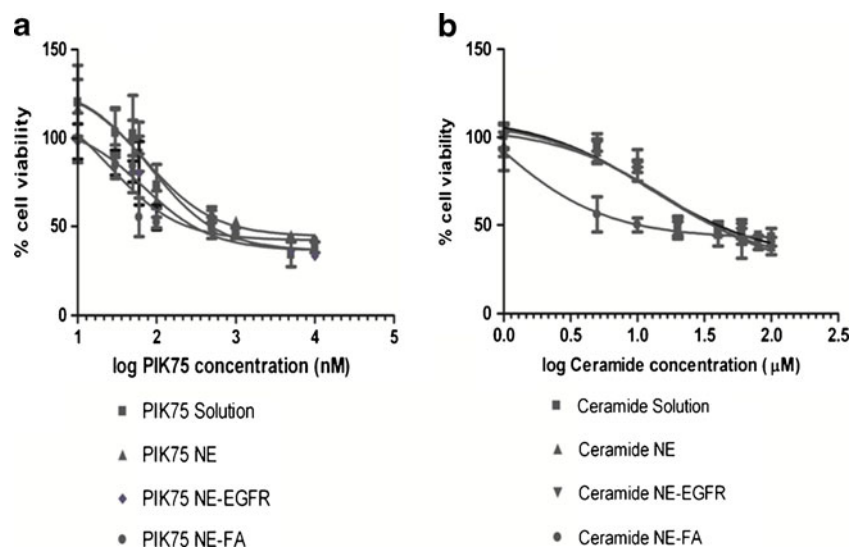


**Table II**  $IC_{50}$  values of PIK75 and Ceramide Formulations in SKOV-3 Cells as Single and Combination Therapy

Formulation	$IC_{50}$ values ( $\mu$ M)
PIK75 solution	$0.301 \pm 4$
PIK75 NE	$0.309 \pm 4$
PIK75 NE-EGFR	$0.170 \pm 3$
PIK75 NE-FA	$0.118 \pm 3$
Ceramide solution	$13 \pm 3$
Ceramide NE	$19 \pm 4$
Ceramide NE-EGFR	$14 \pm 3$
Ceramide NE-FR	$10 \pm 4$
PIK75 + Ceramide in solution	$0.155 \pm 4$
PIK75 + Ceramide in NE	$0.174 \pm 4$
PIK75 + Ceramide in NE-EGFR	$0.103 \pm 4$
PIK75 + Ceramide in NE-FA	$0.105 \pm 4$

Figure 4b shows the percentage cell viability following treatment with ceramide formulations. The ceramide solution and nanoemulsions showed  $IC_{50}$  values between  $10 \mu$ M to  $19 \mu$ M. Statistical analysis indicated a significant difference between targeted and non-targeted ceramide nanoemulsions.

It has been reported that when ceramide is combined with paclitaxel, temporal spacing of these agents provides effective therapy against multiple drug resistant breast and ovarian cancer (32). Hence, prior to conducting the combination study with PIK75 and ceramide, temporal spacing of these agents was investigated to consider the mechanistic action of these individual agents on SKOV-3 cells. Table III shows the percentage cell viability following temporal spacing of PIK75 solution and ceramide solution. Dosing SKOV-3 cells with PIK75 solution and ceramide solution at different intervals showed percentage cell viability between 46-51% indicating temporal spacing of these agents



**Table III** Temporal study of PIK75 and C<sub>6</sub>-ceramide to Determine Dosing Interval of Each Compound in SKOV-3 Cells

Treatment combination	% cell viability
PIK75 <sub>0 h</sub> + Cer <sub>0 h</sub>	48.18 ± 0.63*
PIK75 <sub>0 h</sub> + Cer <sub>2 h</sub>	49.09 ± 1.92
PIK75 <sub>0 h</sub> + Cer <sub>4 h</sub>	49.13 ± 2.64
PIK75 <sub>0 h</sub> + Cer <sub>6 h</sub>	47.72 ± 3.75
PIK75 <sub>2 h</sub> + Cer <sub>0 h</sub>	48.01 ± 3.01
PIK75 <sub>4 h</sub> + Cer <sub>0 h</sub>	50.57 ± 3.07
PIK75 <sub>6 h</sub> + Cer <sub>0 h</sub>	46.29 ± 3.61

\*Mean ± S.D. (n=3)

did not affect percentage cell viability. Hence, combination studies with all the PIK75 and ceramide formulations were conducted with simultaneous dosing of both agents.

Figure 5 illustrates the percentage cell viability following combination of PIK75 and ceramide formulations and Table II shows the corresponding PIK75 IC<sub>50</sub> values. Combination of PIK75 and ceramide resulted in a significant decrease in PIK75 IC<sub>50</sub> values compared to individualized therapy with PIK75 in all formulation systems. Combination therapy with PIK75 and ceramide in NE showed 59%

decrease in IC<sub>50</sub> value of PIK75 compared to the solution form ( $p < 0.05$ ). In contrast to this, both the targeted systems showed 66-68% decrease in PIK75 IC<sub>50</sub> when dosed to SKOV-3 cells as combination therapy. However, there was no significant difference in the IC<sub>50</sub> value of PIK75 following combination therapy with both the targeted systems.

## Qualitative and Quantitative apoptotic analysis

### TUNEL Assay

TUNEL assay is a qualitative test for analysis of cellular apoptosis. In this assay the biotinylated nucleotides are incorporated at 3'-OH DNA end of the fragmented DNA. This is followed by binding of horseradish peroxidase-labeled streptavidin to the incorporated nucleotides. These nucleotides are then detected with the help of peroxidase substrate diaminobenzidine which results in the formation of dark brown stains. Figure 6 shows the untreated cells and cells treated with DMSO and blank nanoemulsion. These cells do not show brown colored nuclei indicating that no apoptosis had occurred. Cells treated with PIK75 and ceramide as single therapy or in combination showed brown color nuclei

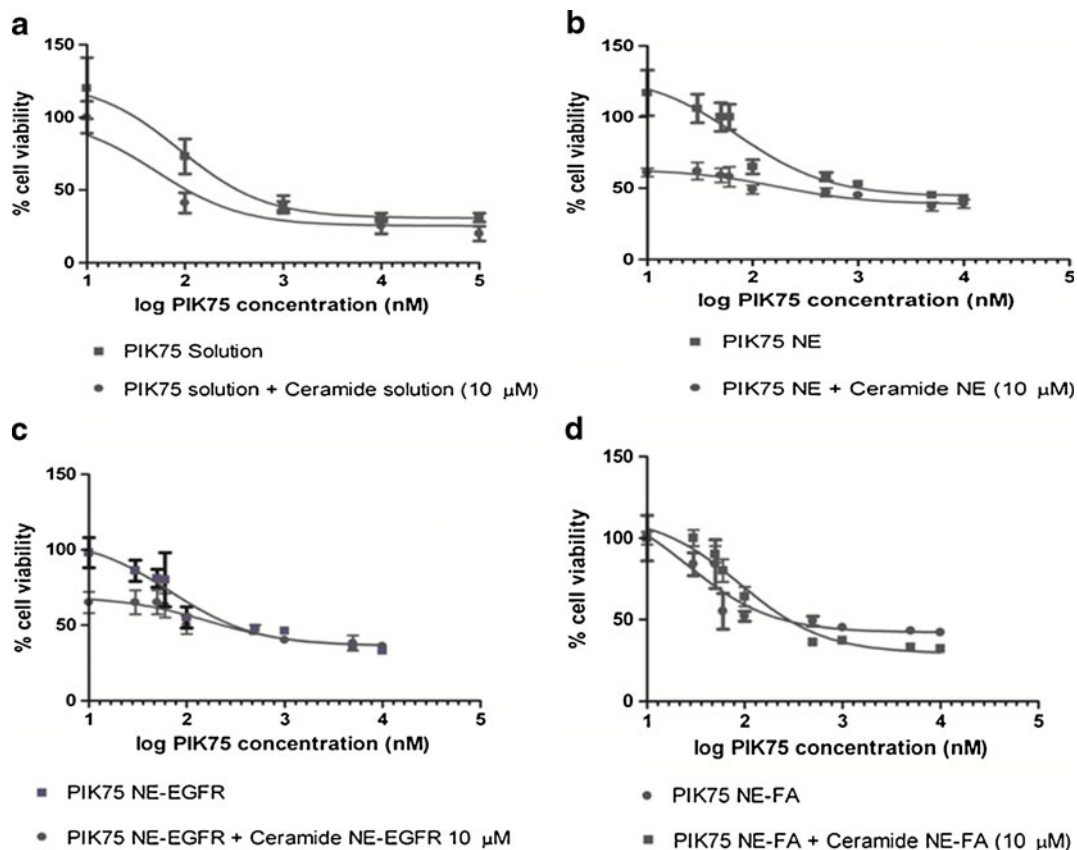


**Fig. 5** Percentage cell viability of SKOV-3 cells in combination study of (a) PIK75 and Ceramide in solution, (b) PIK75 and Ceramide in nanoemulsion, (c) PIK75 and Ceramide in EGFR targeted nanoemulsion, (d) PIK75 and Ceramide in folate targeted nanoemulsion. The results represent mean ± SD, n=8.

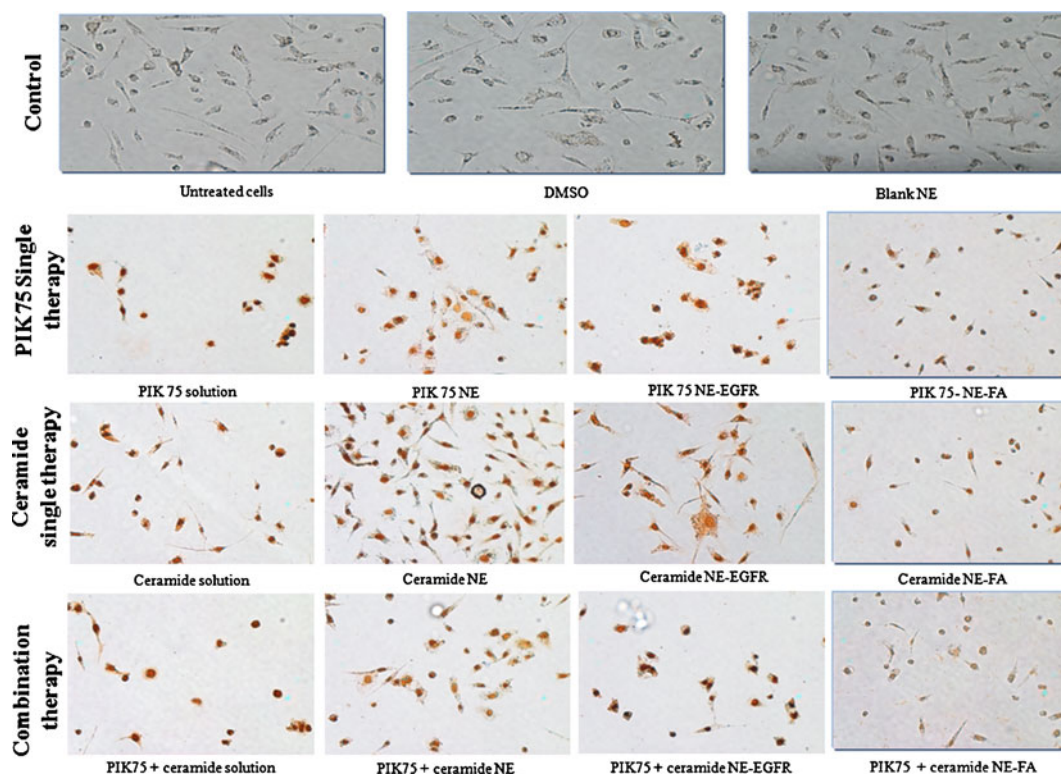


**Fig. 6** TUNEL staining images of SKOV-3 cells treated with PIK75 and ceramide formulations as single and combination therapy. Images obtained at 20 $\times$  magnification.

indicating apoptosis. The cells that were treated with a combination of PIK75 and ceramide showed pronounced dark brown coloration of the nuclei. This correlated with cytotoxicity data (Fig. 5) which indicated that combination therapy showed higher therapeutic efficacy (33).

#### Caspase-3/7 Activity Measurements

Figure 7a, shows the caspase 3/7 activity in SKOV-3 cells following treatment with PIK75 and ceramide as individual and combination treatment. For these studies, PIK75 and ceramide were administered at a concentration of 100 nM and 10  $\mu$ M respectively, individually and in combination. All the PIK75 formulations showed 0.9 to 1.4-fold increase in caspase activity relative to controls. PIK75 NE showed 1.3-fold higher caspase activity while PIK75 NE-FA system showed a 1.5-fold higher caspase activity compared to PIK75 solution ( $p < 0.05$ ).

Combination treatment with ceramide showed an increase in caspase activity with all the formulations. A 1.3- to 1.5-fold improvement in caspase activity was observed with the use of ceramide ( $p < 0.05$ ). These findings support the results observed in TUNEL assay and cell viability studies where combination therapy showed greater cytotoxicity compared to individual therapy with PIK75.

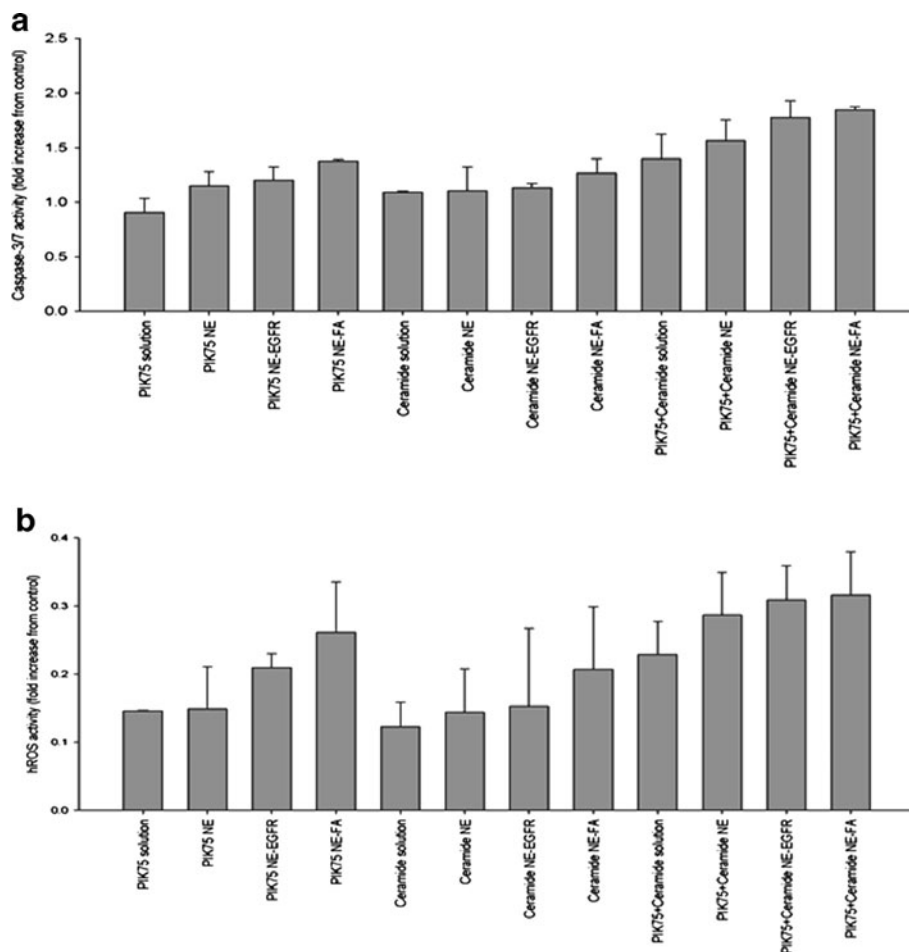
#### Detection of Highly Reactive Oxygen Species Markers Following Treatment with PIK75 Nanoemulsion Formulations

Figure 7b shows the hROS activity based on fluorescent intensity at 10  $\mu$ M dye concentration. All the formulations showed a small increase in hROS activity relative to controls. When SKOV-3 cells were treated with PIK75 formulations as single therapy a 0.1- to 0.3-fold increase in hROS activity was detected relative to controls. On the other hand, a statistically significant increase in hROS activity was detected when SKOV-3 cells were treated with a combination of PIK75 and ceramide. This indicated that an improvement in cell cytotoxicity following combination therapy with PIK75 and ceramide could be attributed to enhanced apoptosis and also by a small increase in hROS markers in cells.

#### DISCUSSION

Nanoemulsions are thermodynamically stable systems comprising of two immiscible liquid phases stabilized with an appropriate stabilizer. Due to the ability of these systems to incorporate lipid vehicle surrounded by an aqueous phase, lipophilic compounds can be incorporated in the core of

**Fig. 7** (a) Quantitative pro-apoptotic analysis using ApoONE Caspase 3/7 activity measurements in SKOV-3 cells following treatment with PIK75 and ceramide as individual and combination treatment. The results represent mean  $\pm$  SD,  $n=3$ . (b) hROS activity following incubation with PIK75 and ceramide formulation as individual treatment and in combination. Each treatment represents  $n=3$ .



these delivery systems. These delivery systems have been investigated for the delivery of several anticancer agents with poor aqueous solubility (18,19,33–35).

In this study PIK75, a poorly water-soluble anticancer agent was solubilized in flaxseed oil and made into nanoemulsion formulations using high-energy ultrasonication process. The surface of these systems was coated with poly (ethylene) glycol to prevent rapid uptake of the nanoemulsion by reticuloendothelial cells, which would enhance residence time and improve accumulation in tumors by the enhanced permeation retention effect (36). Surface functionalization of the nanoemulsions was achieved by incorporating EGF peptide and folic acid in the nanoemulsions to target receptors that are usually highly expressed in several tumors and have been investigated for the targeted delivery of nanoparticles (21–23). SKOV-3 cells are human ovarian adenocarcinoma cells with increased EGFR and FR expression on their cell surface (21,37). The p110  $\alpha$  isoform of PI3K enzyme is frequently activated in these cell lines (38) and hence these cells were investigated for the delivery of PIK75 in nanoemulsion formulations.

Non-targeted and targeted nanoemulsions were prepared using the ultrasonication technique. This technique enabled the preparation of spherical nanoemulsions (Fig. 1) with a

size below 250 nm and a uniform particle size distribution (Table II). Surface functionalization of the nanoemulsions with the EGF peptide (GE11) or folic acid did not affect particle size distribution of the nanoemulsions (Table I). The zeta potential value indicates the degree of ionization of the components adsorbed at the interfacial layer of the nanoemulsions. The egg lecithin, which was used as a stabilizer in the nanoemulsion provided the negative surface charge value in the range of (–) 51.83 to (–) 58.03 mV.

Using the ultrasonication technique, PIK75 and ceramide nanoemulsions (non-targeted, as well as EGFR or FR targeted) were prepared and investigated as individual therapy and combination therapy in SKOV-3 cells. The qualitative cellular uptake analysis with NBD-C<sub>6</sub> ceramide indicates that both targeted and non-targeted nanoemulsions were efficiently internalized by SKOV-3 cells (Fig. 2). Both the non-targeted and the targeted systems showed cellular uptake of NBD-C<sub>6</sub> ceramide within 15 min of incubation but higher fluorescence intensity was observed only for the targeted systems. Hence quantitative cellular uptake studies were conducted by incubating the SKOV-3 cells with PIK75 formulations at an interval of 1 and 6 h to determine if PIK75 would have greater uptake from the targeted nanoemulsions compared to non-targeted

nanoemulsions. The concentration of PIK75 detected after 1 h incubation time was below the limit of quantitation of the assay and therefore only 6 h incubation time points were analyzed.

Quantitative cellular uptake studies with PIK75 indicated that the non-targeted nanoemulsions showed greater uptake of PIK75 compared to PIK75 solution. Both the targeted systems showed a statistically significant increase in uptake of PIK75, which indicated that higher subcellular levels of PIK75 were achieved by formulating PIK75 in targeted nanoemulsions.

Cytotoxicity assays were conducted to determine if a higher subcellular concentration of PIK75 would lead to a decrease in cell viability. When PIK75 was administered in single therapy the targeted nanoemulsions showed a significant improvement in cytotoxicity compared to PIK75 solution and PIK75 NE. These results correlate well with the quantitative uptake data where a higher concentration of PIK75 was detected in SKOV-3 cells using the targeted nanoemulsion compared to non-targeted nanoemulsion. EGFR and FR targeted nanoemulsions would be taken into the cells by specific receptor mediated endocytosis in contrast to non-specific uptake of non-targeted nanoemulsions (39). With EGF mediated systems, this process occurs within 10 to 20 min of stimulation (40). It has also been observed that since the uptake of these systems is receptor mediated, these systems can bypass cancer cell multi-drug efflux pumps (39). Hence, the enhanced uptake with the targeted system can lead to greater cytotoxicity.

Combination therapy with ceramide has been reported to give improvements in cytotoxicity for many polymeric nanoparticles (28,29,32). In the present study, combination of PIK75 and ceramide enhanced PIK75 cytotoxicity compared to individualized treatment. PIK75 exhibits cytotoxic activity by inhibiting the PI3K enzyme thus preventing cell growth and proliferation (11). Ceramide is known to enhance cellular apoptosis by activating the intrinsic and extrinsic apoptotic pathway (41). Due to the varied mechanism of these agents their co-administration would enable them to act synergistically leading to improved cytotoxicity.

Qualitative and quantitative analysis of apoptosis was conducted using the TUNEL assay and Caspase-3/7 assay respectively and suggested that the increased cell cytotoxicity could be attributed to increased cellular apoptosis. Several authors have observed that PI3K activates AKT/PKB which possibly leads to inhibition of caspase activity (42–44). Hence the enhanced apoptosis observed with the PIK75 nanoemulsions could be due to the effect of PIK75 on the PI3K pathway leading to increase in caspase activity.

hROS are chemically reactive oxygen species which are formed as a byproduct of normal metabolism of oxygen and these have important roles in cell signaling and homeostasis. During times of environmental stress (e.g. exposure to

chemotherapeutic agents) ROS levels can increase dramatically resulting in damage to cell structures. Hence, in this study, measurement of hROS markers also indicated a slight increase in hROS activity with some formulations. This indicated that other pathways were also contributing to improved cytotoxicity in SKOV-3 cells.

## CONCLUSION

Nanoemulsions containing PIK75, ceramide and combination of PIK75 and ceramide were successfully prepared using ultrasonication technique with a size below 250 nm. These formulations were surface functionalized for targeted drug delivery to ovarian cancer cells. Targeted and non-targeted nanoemulsions were delivered inside SKOV-3 cells and provided enhanced cytotoxicity. The increase in cytotoxicity was attributed to an increase in apoptosis and also due to a small increase in hROS activity especially in combination therapy with PIK75 and ceramide. The results of this study demonstrate a therapeutic benefit of incorporating PIK75 in targeted nanoemulsion. Further, co-administration of PIK75 and ceramide could provide further benefits by allowing these agents to work on multiple pathways simultaneously to produce greater cytotoxic effect. Further *in vivo* studies in human xenograft models will be required to confirm the benefits of this system *in vivo*.

## ACKNOWLEDGMENTS AND DISCLOSURES

Meghna Talekar thanks the University of Auckland Scholarship office and Lottery Health Research Committee for support.

## REFERENCES

1. Society AC. Ovarian Cancer. 2012; Available from: <http://www.cancer.org/Cancer/OvarianCancer/DetailedGuide/ovarian-cancer-key-statistics>.
2. Gymnopoulos M, Elsliger MA, Vogt PK. Rare cancer-specific mutations in PIK3CA show gain of function. *Proc Natl Acad Sci U S A*. 2007;104(13):5569–74.
3. Bader AG, Kang S, Vogt PK. Cancer-specific mutations in PIK3CA are oncogenic *in vivo*. *Proc Natl Acad Sci U S A*. 2006;103(5):1475–9.
4. Frédéric R, Mawson C, Kendall JD, Chaussade C, Rewcastle GW, Shepherd PR, Denny WA. Phosphoinositide-3-kinase (PI3K) inhibitors: Identification of new scaffolds using virtual screening. *Bioorg Med Chem Lett*. 2009;19(20):5842–7.
5. Hu L, Hofmann J, Lu Y, Mills GB, Jaffe RB. Inhibition of phosphatidylinositol 3'-kinase increases efficacy of paclitaxel in *in vitro* and *in vivo* ovarian cancer models. *Cancer Res*. 2002;62(4):1087–92.
6. Karakas B, Bachman KE, Park BH. Mutation of the PIK3CA oncogene in human cancers. *Br J Cancer*. 2006;94(4):455–9.

7. Marone R, Cmiljanovic V, Giese B, Wymann M. Targeting phosphoinositide 3-kinase--Moving towards therapy. *Biochim Biophys Acta Protein Proteomics*. 2008;1784(1):159–85.
8. Hirsch E, Ciraoalo E, Ghigo A, Costa C. Taming the PI3K team to hold inflammation and cancer at bay. *Pharmacol Ther*. 2008;118(2):192–205.
9. Maira SM, Voliva C, Garcia-Echeverria C. Class IA phosphatidylinositol 3-kinase: from their biologic implication in human cancers to drug discovery. *Expert Opin Ther Targets*. 2008;12(2):223–38.
10. Knight ZA, Gonzalez B, Feldman ME, Zunder ER, Goldenberg DD, Williams O, Loewith R, Stokoe D, Balla A, Toth B, Balla T, Weiss WA, Williams RL, Shokat KM. A Pharmacological map of the PI3-K family defines a role for p110 $\alpha$  in insulin signaling. *Cell*. 2006;125(4):733–47.
11. Chaussade C, Rewcastle GW, Kendall JD, Denny WA, Cho K, Gronning LM, Chong ML, Anagnostou SH, Jackson SP, Daniele N, Shepherd PR. Evidence for functional redundancy of class IA PI3K isoforms in insulin signalling. *Biochem J*. 2007;404(3):449–58.
12. Kendall JD, Rewcastle GW, Frederick R, Mawson C, Denny WA, Marshall ES, Baguley BC, Chaussade C, Jackson SP, Shepherd PR. Synthesis, biological evaluation and molecular modelling of sulfonohydrazides as selective PI3K p110[ $\alpha$ ] inhibitors. *Bioorg Med Chem*. 2007;15(24):7677–87.
13. Hayakawa M, Kawaguchi KI, Kaizawa H, Koizumi T, Ohishi T, Yamano M, Okada M, Ohta M, Tsukamoto SI, Raynaud FI, Parker P, Workman P, Waterfield MD. Synthesis and biological evaluation of sulfonylhydrazone-substituted imidazo[1,2-*a*]pyridines as novel PI3 kinase p110 $\alpha$  inhibitors. *Bioorg Med Chem*. 2007;15(17):5837–44.
14. Dagia NM, Agarwal G, Kamath DV, Chetrapal-Kunwar A, Gupte RD, Jadhav MG, Dadarkar SS, Trivedi J, Kulkarni-Almeida AA, Kharas F, Fonseca LC, Kumar S, Bhonde MR. A preferential p110 $\alpha$ / $\gamma$  PI3K inhibitor attenuates experimental inflammation by suppressing the production of proinflammatory mediators in a NF- $\kappa$ B-dependent manner. *Am J Physiol Cell Physiol*. 2010;298(4):C929–41.
15. Tiwari SB, Amiji MM. Improved oral delivery of paclitaxel following administration in nanoemulsion formulations. *J Nanosci Nanotechnol*. 2006;6(9–10):3215–21.
16. Lo Prete AC, Maria DA, Rodrigues DG, Valduga CJ, Ibañez OCM, Maranhão RC. Evaluation in melanoma-bearing mice of an etoposide derivative associated to a cholesterol-rich nanoemulsion. *J Pharm Pharmacol*. 2006;58(6):801–8.
17. Ohguchi Y, Kawano K, Hattori Y, Maitani Y. Selective delivery of folate-PEG-linked, nanoemulsion-loaded aclacinomycin A to KB nasopharyngeal cells and xenograft: Effect of chain length and amount of folate-PEG linker. *J Drug Target*. 2008;16(9):660–7.
18. Tagne JB, Kakumanu S, Nicolosi RJ. Nanoemulsion preparations of the anticancer drug dacarbazine significantly increase its efficacy in a xenograft mouse melanoma model. *Mol Pharm*. 2008;5(6):1055–63.
19. Tagne JB, Kakumanu S, Ortiz D, Shea T, Nicolosi RJ. A nanoemulsion formulation of tamoxifen increases its efficacy in a breast cancer cell line. *Mol Pharm*. 2008;5(2):280–6.
20. Kawakami S, Yamashita F, Hashida M. Disposition characteristics of emulsions and incorporated drugs after systemic or local injection. *Adv Drug Deliv Rev*. 2000;45(1):77–88.
21. Milane L, Duan Z, Amiji M. Development of EGFR-targeted polymer blend nanocarriers for combination paclitaxel/lonidamine delivery to treat multi-drug resistance in human breast and ovarian tumor cells. *Mol Pharm*. 2011;8(1):185–203.
22. Magadala P, Amiji M. Epidermal growth factor receptor-targeted gelatin-based engineered nanocarriers for DNA delivery and transfection in human pancreatic cancer cells. *AAPS J*. 2008;10(4):565–76.
23. Liu Y, Sun J, Cao W, Yang J, Lian H, Li X, Sun Y, Wang Y, Wang S, He Z. Dual targeting folate-conjugated hyaluronic acid polymeric micelles for paclitaxel delivery. *Int J Pharm*. 2011;421(1):160–9.
24. Kang C, Yuan X, Zhong Y, Pu P, Guo Y, Albadany A, Yu S, Zhang Z, Li Y, Chang J, Sheng J. Evaluation of folate-PAMAM for the delivery of antisense oligonucleotides to rat C6 glioma cells *in vitro* and *in vivo*. *J Biomed Mater Res*. 2010;93(2):585–94.
25. Leamon CP, Low PS. Selective targeting of malignant cells with cytotoxin-folate conjugates. *J Drug Target*. 1994;2(2):101–12.
26. Asadishad B, Vossoughi M, Alemzadeh I. Folate-receptor-targeted delivery of doxorubicin using polyethylene glycol-functionalized gold nanoparticles. *Ind Eng Chem Res*. 2010;49(4):1958–63.
27. Huang W, Chen C., Lin Y, Lin C. Apoptotic sphingolipid ceramide in cancer therapy. *Journal of Lipids*. 2011;2011.
28. Van Vlerken LE, Duan Z, Little SR, Seiden MV, Amiji MM. Modulation of intracellular ceramide using polymeric nanoparticles to overcome multidrug resistance in cancer. *Cancer Res*. 2007;67(10):4843–50.
29. Devalapally H, Duan Z, Seiden MV, Amiji MM. Paclitaxel and ceramide co-administration in biodegradable polymeric nanoparticulate delivery system to overcome drug resistance in ovarian cancer. *Int J Cancer*. 2007;121(8):1830–8.
30. Li Z, Zhao R, Wu X, Sun Y, Yao M, Li J, Xu Y, Gu J. Identification and characterization of a novel peptide ligand of epidermal growth factor receptor for targeted delivery of therapeutics. *FASEB J*. 2005;19(14):1978–85.
31. Song S, Liu D, Peng J, Sun Y, Li Z, Gu JR, Xu Y. Peptide ligand-mediated liposome distribution and targeting to EGFR expressing tumor *in vivo*. *Int J Pharm*. 2008;363(1–2):155–61.
32. van Vlerken LE, Duan Z, Little SR, Seiden MV, Amiji MM. Biodistribution and pharmacokinetic analysis of paclitaxel and ceramide administered in multifunctional polymer-blend nanoparticles in drug resistant breast cancer model. *Mol Pharm*. 2008;5(4):516–26.
33. Ganta S, Amiji M. Coadministration of paclitaxel and curcumin in nanoemulsion formulations to overcome multidrug resistance in tumor cells. *Mol Pharm*. 2009;6(3):928–39.
34. Ganta S, Devalapally H, Amiji M. Curcumin enhances oral bioavailability and anti-tumor therapeutic efficacy of paclitaxel upon administration in nanoemulsion formulation. *J Pharm Sci*. 2010;99(11):4630–41.
35. Ganta S, Paxton JW, Baguley BC, Garg S. Pharmacokinetics and pharmacodynamics of chlorambucil delivered in parenteral emulsion. *Int J Pharm*. 2008;360(1–2):115–21.
36. Talekar M, Kendall J, Denny W, Garg S. Targeting of nanoparticles in cancer: drug delivery and diagnostics. *Anti Canc Drugs*. 2011;22(10):949–62.
37. Werner ME, Karve S, Sukumar R, Cummings ND, Copp JA, Chen RC, Zhang T, Wang AZ. Folate-targeted nanoparticle delivery of chemo- and radiotherapeutics for the treatment of ovarian cancer peritoneal metastasis. *Biomaterials*. 2011;32(33):8548–54.
38. Shayesteh L, Lu Y, Kuo WL, Baldocchi R, Godfrey T, Collins C, Pintel D, Powell B, Mills GB, Gray JW. PIK3CA is implicated as an oncogene in ovarian cancer. *Nat Genet*. 1999;21(1):99–102.
39. Esmaceli F, Ghahremani MH, Ostad SN, Atyabi F, Seyedabadi M, Malekshahi MR, Amini M, Dinarvand R. Folate-receptor-targeted delivery of docetaxel nanoparticles prepared by PLGA-PEG-folate conjugate. *J Drug Target*. 2008;16(5):415–23.
40. Orth JD, Krueger EW, Weller SG, McNiven MA. A novel endocytic mechanism of epidermal growth factor receptor sequestration and internalization. *Cancer Res*. 2006;66(7):3603–10.
41. Thevissen K, François IEJA, Winderickx J, Pannecouque C, Cammue BPA. Ceramide involvement in apoptosis and apoptotic diseases. *Mini-Reviews in Medicinal Chem*. 2006;6(6):699–709.